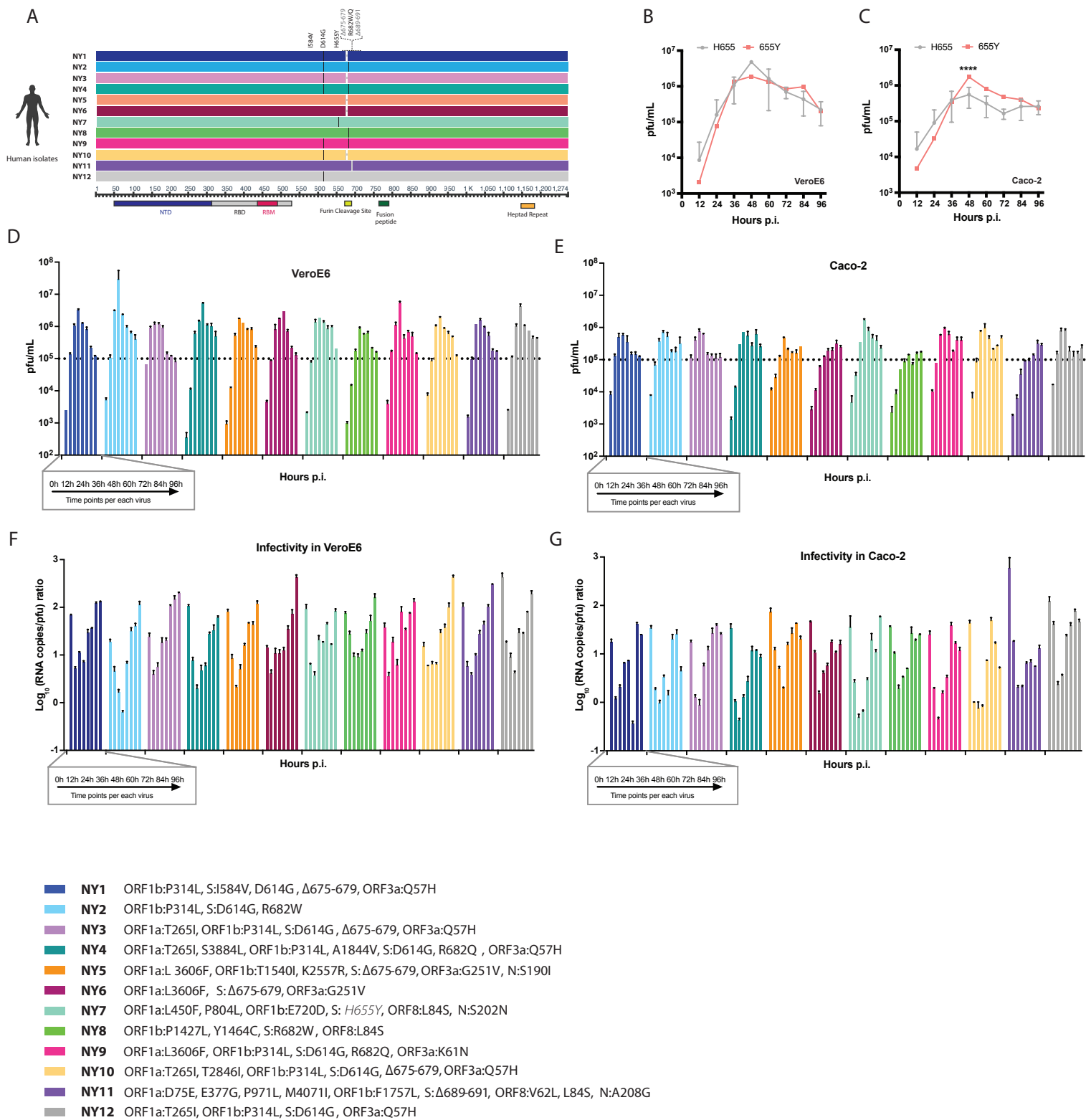
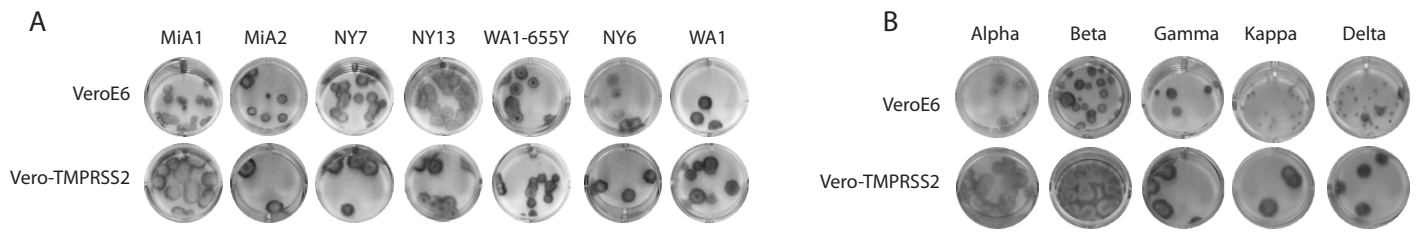


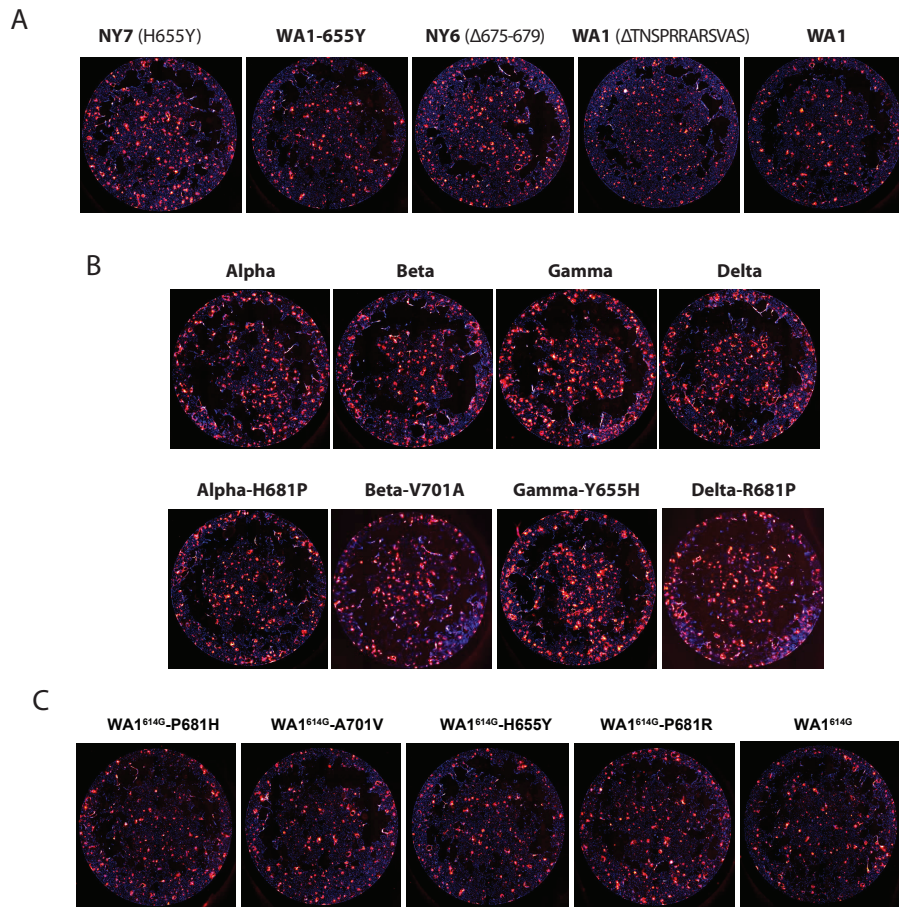
Supplementary Figure 1 related to Methods and Figure 2. Spike polymorphism H655Y is selected after SARS-CoV-2 replication in mink in vivo model. A) Mink study design: six minks were infected with 10^6 pfu of SARS-CoV-2 WA1 isolate. Nasal washes were collected at day 1, 3 and 5 post-infection (p.i.) and organs were harvested at day 3 and 7 p.i. **B)** Viral titers of nasal washes expressed as PFU per milliliter. **C)** Organ viral titers expressed as pfu per gram of tissue. **D)** Multiple sequence alignment of the spike (S) protein from SARS-CoV-2 viruses isolated after infection in minks with WA1 isolate. Diagram shows the corresponding S amino acid substitutions mapped to the S gene.



Supplementary Figure 2 related to Figure 1 and Figure 2. Spike polymorphism H655Y identified in SARS-CoV-2 NY7 confers a growth advantage in human Caco-2 cells. A) Multiple sequence alignment of the S protein from SARS-CoV-2 viruses isolated from nasal swabs collected during the first pandemic wave in NY. Diagram shows the corresponding S amino acid substitutions mapped to the S gene. **B-C)** Viral growth of the NY7 containing the 655Y (red) versus its ancestors 655H (grey) in VeroE6 and Caco-2 cells. Cells were infected at an MOI of 0.01 and supernatants were titrated in duplicates at the indicated hours post-infection (p.i.) and expressed as plaque forming units per milliliter (PFU). Means and SD are shown for the NY isolates containing 655H. Two-way ANOVA with Holm-Šidák posttest was used for multiple comparisons. Statistical significance was considered when $p \leq 0.05$ (****, $p < 0.0001$). Replication kinetics of 12 NY human isolates in **D)** VeroE6 and **E)** Caco-2 cells. Cells were infected at a multiplicity of infection (MOI) of 0.01. Viral titers were determined by plaque assay and expressed as PFU per milliliter at the indicated hours post-infection (p.i.). Means and range are shown from two independent experiments. Virion infectivity expressed as genomic RNA/pfu ratio in **F)** VeroE6 and **G)** Caco-2 cells. Cells were infected at a MOI of 0.01. The genomic viral RNA was determined by RT-qPCR. Means and range are shown from two independent experiments.



Supplementary Figure 3 related to Figure 2 and Figure 6. Plaque phenotype of A) early SARS-CoV-2 isolates and B) VOCs according to TMPRSS2 expression in Vero cells. The same viral supernatant was used to infect Vero and Vero-TMPRSS2 cells. Plaques were developed by immunostaining.



Supplementary Figure 4 related to Figure 3 and Figure 7. Spike expression levels of SARS-CoV-2 isolates in split-GFP fusion assay. Vero-TMPRSS2 cells were transfected with Spike plasmids from **A)** the early SARS-CoV-2 isolates, **B)** VOCs and reverse mutants and **C)** gain of function mutants in WA1-D614G backbone. Cells were stained against Spike protein and DAPI was used to visualize the nucleus. Images of the whole wells were obtained and analyzed using the Celigo Image Cytometer (Nexcelom).

Supplementary Table 1 related to Methods and Figure 1. GISAID accession numbers of human SARS-CoV-2 variants isolated from New York (NY) during the first COVID-19 pandemic outbreak.

SARS-CoV-2 isolate	GISAID accession number
NY1	HCOV19/NY/PV08139/2020_EPI_ISL_MSPV08139
NY2	HCOV19/NY/PV08426/2020_EPI_ISL_MSPV08426
NY3	HCOV19/NY/PV08428/2020_EPI_ISL_MSPV08428
NY4	HCOV19/NY/PV08485/2020_EPI_ISL_MSPV08485
NY5	HCOV19/NY/PV08137/2020_EPI_ISL_MSPV08137
NY6	HCOV19/NY/PV08489/2020_EPI_ISL_MSPV08489
NY7	HCOV19/NY/PV08148/2020_EPI_ISL_MSPV08148
NY8	HCOV19/NY/PV08146/2020_EPI_ISL_MSPV08146
NY9	HCOV19/NY/PV08462/2020_EPI_ISL_MSPV08462
NY10	HCOV19/NY/PV08468/2020_EPI_ISL_MSPV08468
NY11	HCOV19/NY/PV08490/2020_EPI_ISL_MSPV08490
NY12	HCOV19/NY/PV08495/2020_EPI_ISL_MSPV08495

Supplementary Table 2 related to Figure 1 and Figure 2. Genomic mutations of mink-derived SARS-CoV-2 isolates (MiA) and human SARS-CoV-2 circulating variants during the first pandemic outbreak in New York (NY).

SARS-CoV-2 isolate	Mutations
MiA-1	ORF1a:S692P, S:T259K, <u>H655Y</u> , H1159Y, ORF8:L84S
MiA-2	S:T259K, <u>H655Y</u> , H1159Y, ORF8:L84S
MiA-3	S:T259K, <u>H655Y</u> , ORF6:F22*, ΔK23, ORF8:L84S
MiA-4	S: <u>H655Y</u> , R682W, ORF8:L84S
MiA-5	ORF1a:L3606F, S: <u>H655Y</u> , R682W, ORF8:L84S
MiA-6	S: <u>H655Y</u> , R682W, ORF8:L84S
NY1	ORF1b:P314L, S:I584V, D614G, Δ675-679, ORF3a:Q57H
NY2	ORF1b:P314L, S:D614G, R682W
NY3	ORF1a:T265I, ORF1b:P314L, S:D614G, Δ675-679, ORF3a:Q57H
NY4	ORF1a:T265I, S3884L, ORF1b:P314L, A1844V, S:D614G, R682Q, ORF3a:Q57H
NY5	ORF1a:L3606F, ORF1b:T1540I, K2557R, S:Δ675-679, ORF3a:G251V, N:S190I
NY6	ORF1a:L3606F, S:Δ675-679, ORF3a:G251V
NY7	ORF1a:L450F, P804L, ORF1b:E720D, S: <u>H655Y</u> , ORF8:L84S, N:S202N
NY8	ORF1b:P1427L, Y1464C, S:R682W, ORF8:L84S
NY9	ORF1a:L3606F, ORF1b:P314L, S:D614G, R682Q, ORF3a:K61N
NY10	ORF1a:T265I, T2846I, ORF1b:P314L, S:D614G, Δ675-679, ORF3a:Q57H
NY11	ORF1a:D75E, E377G, P971L, M4071I, ORF1b:F1757L, S:Δ689-691, ORF8:V62L, L84S, N:A208G
NY12	ORF1a:T265I, ORF1b:P314L, S:D614G, ORF3a:Q57H

Supplementary Table 3 related to Methods. Primers used to detect SARS-CoV-2 RNA in nasopharyngeal swabs from COVID-19 infected patients.

Primer	Nucleotide sequence 5'>3'
2019-nCoV_N1 Forward Primer	GAC CCC AAA ATC AGC GAA AT
2019-nCoV_N1 Reverse Primer	TCT GGT TAC TGC CAG TTG AAT CTG
2019-nCoV_N2 Forward Primer	TTA CAA ACA TTG GCC GCA AA
2019-nCoV_N2 Reverse Primer	GCG CGA CAT TCC GAA GAA

Supplementary Table 4 related to Figure 2. Multiple comparison analysis of the viral growth of the panel of 655Y viruses used in this study.

	Tukey's multiple comparisons test	Mean Diff.	95.00% CI of diff.	Summary	Adjusted P Value
VeroE6 24h p.i.	MiA1 vs. NY13	1133333	37431 to 2229235	*	0.0406
	MiA1 vs. WA1 wt	1275000	179098 to 2370902	*	0.0182
	MiA2 vs. WA1 wt	1208333	112431 to 2304235	*	0.0266
	WA1-655Y vs. WA1 wt	1175000	79098 to 2270902	*	0.0321
Vero-TMPRSS2 24h p.i.	MiA2 vs. WA1 wt	3958333	104340 to 7812326	*	0.0424
Vero-TMPRSS2 48h p.i.	MiA1 vs. WA1-655Y	-6016667	-11530583 to -502750	*	0.0286
	MiA2 vs. WA1-655Y	-6316667	-11830583 to -802750	*	0.0204
Pneumocytes 24h p.i.	NY7 vs. NY13	-46667	-68524 to -24809	***	0.0003
	NY7 vs. WA1-655Y	-26667	-48524 to -4809	*	0.0163
	NY7 vs. NY6	-48333	-70191 to -26476	***	0.0002
	NY13 vs. WA1 wt	55583	33726 to 77441	****	<0.0001
	WA1-655Y vs. WA1 wt	35583	13726 to 57441	**	0.0023
	NY6 vs. WA1 wt	57250	35393 to 79107	****	<0.0001

Supplementary Table 5 related to Figure 6. Multiple comparison analysis of the viral growth of the VOCs used in this study.

	Tukey's multiple comparisons test	Mean Diff.	95.00% CI of diff.	Summary	Adjusted P Value
VeroE6 24h p.i.	Alpha vs. Beta	-1368333	-1735453 to -1001213	****	<0.0001
	Beta vs. Gamma	1296667	929547 to 1663787	****	<0.0001
	Beta vs. Kappa	1431450	1064330 to 1798570	****	<0.0001
	Beta vs. Delta	1412167	1045047 to 1779287	****	<0.0001
VeroE6 48h p.i.	Alpha vs. Kappa	4225000	529473 to 7920527	*	0.0241
	Beta vs. Gamma	5033333	1337806 to 8728860	**	0.0081
	Beta vs. Kappa	6725000	3029473 to 10420527	***	0.001
	Beta vs. Delta	5400000	1704473 to 9095527	**	0.005
Vero-TMPRSS2 24h p.i.	Alpha vs. Beta	-1603333	-2297761 to -908905	***	0.0001
	Alpha vs. Gamma	-970000	-1664428 to -275572	**	0.0068
	Beta vs. Kappa	1610000	915572 to 2304428	***	0.0001
	Beta vs. Delta	1640000	945572 to 2334428	***	0.0001
	Gamma vs. Kappa	976667	282239 to 1671095	**	0.0065
	Gamma vs. Delta	1006667	312239 to 1701095	**	0.0053
Vero-TMPRSS2 48h p.i.	Beta vs. Gamma	-2433333	-4478858 to -387808	*	0.019
	Gamma vs. Kappa	3386667	1341142 to 5432192	**	0.002
	Gamma vs. Delta	3405000	1359475 to 5450525	**	0.0019
Pneumocytes 24h p.i.	Alpha vs. Beta	-138333	-162234 to -114433	****	<0.0001
	Alpha vs. Gamma	-35000	-58901 to -11099	**	0.0049
	Alpha vs. Kappa	55450	31549 to 79351	***	0.0001
	Alpha vs. Delta	53383	29483 to 77284	***	0.0002
	Beta vs. Gamma	103333	79433 to 127234	****	<0.0001
	Beta vs. Kappa	193783	169883 to 217684	****	<0.0001
	Beta vs. Delta	191717	167816 to 215617	****	<0.0001
	Gamma vs. Kappa	90450	66549 to 114351	****	<0.0001
	Gamma vs. Delta	88383	64483 to 112284	****	<0.0001
Pneumocytes 48h p.i.	Beta vs. Kappa	3953333	635648 to 7271019	*	0.0188
	Beta vs. Delta	3961667	643981 to 7279352	*	0.0186

Supplementary Table 6 related to Figure 4. Relative abundance of S:655Y on the viral RNA present in the input, nasal washes, lungs, and nasal turbinates of the hamsters analyzed by next-generation sequencing.

Input			56% 655H: 44% 655Y
Sample	Day p.i.	Tissue	% of 655Y
H# Cage 1 ●	2	Nasal washes	98%
H# Cage 1	2	Nasal washes	100%
H# Cage 2 ●	2	Nasal washes	100%
H# Cage 2	2	Nasal washes	99%
H# Cage 3 ●	2	Nasal washes	99%
H# Cage 3	2	Nasal washes	100%
H# Cage 4 ●	2	Nasal washes	99%
H# Cage 4	2	Nasal washes	32%
H# Cage 5 ●	2	Nasal washes	99%
H# Cage 5	2	Nasal washes	99%
H# Cage 1 ●	4	Nasal washes	100%
H# Cage 1	4	Nasal washes	100%
H# Cage 2 ●	4	Nasal washes	Dead
H# Cage 2	4	Nasal washes	99% T
H# Cage 3 ●	4	Nasal washes	99%
H# Cage 3	4	Nasal washes	100%
H# Cage 4 ●	4	Nasal washes	98%
H# Cage 4	4	Nasal washes	29%
H# Cage 5 ●	4	Nasal washes	98%
H# Cage 5	4	Nasal washes	100%
H# Cage 1	6	Nasal washes	100%
H# Cage 2	6	Nasal washes	99%
H# Cage 3	6	Nasal washes	100%
H# Cage 4	6	Nasal washes	15%
H# Cage 5	6	Nasal washes	100%
H# Cage 1 ●	5	Lungs	99%
H# Cage 1	7	Lungs	83%
H# Cage 2 ●	5	Lungs	Dead
H# Cage 2	7	Lungs	No amplification
H# Cage 3 ●	5	Lungs	97%
H# Cage 3	7	Lungs	100%
H# Cage 4 ●	5	Lungs	98%
H# Cage 4	7	Lungs	39%
H# Cage 5 ●	5	Lungs	No amplification
H# Cage 5	7	Lungs	99%
H# Cage 1 ●	5	Nasal turbinates	100%
H# Cage 1	7	Nasal turbinates	No amplification
H# Cage 2 ●	5	Nasal turbinates	Dead
H# Cage 2	7	Nasal turbinates	98%
H# Cage 3 ●	5	Nasal turbinates	No amplification
H# Cage 3	7	Nasal turbinates	100%
H# Cage 4 ●	5	Nasal turbinates	100%
H# Cage 4	7	Nasal turbinates	52%
H# Cage 5 ●	5	Nasal turbinates	100%
H# Cage 5	7	Nasal turbinates	100%

● indicates Direct Infected (DI) animal